Protein phosphatase 1 and an opposing protein kinase regulate steady-state L-type Ca^{2+} current in mouse cardiac myocytes

William H. duBell and Terry B. Rogers

Department of Biochemistry and Molecular Biology, University of Maryland School of Medicine, Baltimore, MD 21201, USA

Studies have suggested that integration of kinase and phosphatase activities maintains the steady-state L-type Ca^{2+} current in ventricular myocytes, a balance disrupted in failing hearts. As we have recently reported that the PP1/PP2A inhibitor calyculin A evokes pronounced increases in L-type I_{Ca}, the goal of this study was to identify the counteracting kinase and phosphatase that determine 'basal' I_{Ca} in isolated mouse ventricular myocytes. Whole-cell voltage-clamp studies, with filling solutions containing 10 mM EGTA, revealed that calyculin A (100 nM) increased I_{Ca} at test potentials between −42 and +49 mV (44% at 0 mV) from a holding potential of −80 mV. It also shifted the $V_{0.5}$ (membrane potential at half-maximal) of both activation (from −17 to −25 mV) and steady-state inactivation (from −32 to −37 mV) in the hyperpolarizing direction. The broad-spectrum protein kinase inhibitor, staurosporine (300 nM), was without effect on I_{Ca} when added after calyculin A. However, by itself, staurosporine decreased I_{Ca} throughout the voltage range examined (50% at 0 mV) and blocked the response to calyculin A, indicating that the phosphatase inhibitor's effects depend upon an opposing kinase activity. The PKA inhibitors Rp-cAMPs (100 μM in the pipette) and H89 (1 μM) failed to reduce basal I_{Ca} or to block the calyculin A-evoked increase in I_{Ca}. Likewise, calyculin A was still active with 10 mM intracellular BAPTA or when Ba^{2+} was used as the charge carrier. These data eliminate roles for protein kinase A (PKA) and calmodulin-dependent protein kinase II (CaMKII) as counteracting kinases. However, the protein kinase C (PKC) inhibitors Ro 31-8220 (1 μM) and Gö 6976 (200 nM) decreased steady-state I_{Ca} and blunted the effect of calyculin A. PP2A is not involved in this regulation as intracellular applications of 10–100 nM okadaic acid or 500 nM fostriecin failed to increase I_{Ca}. However, PP1 is important, as dialysis with 2 μM okadaic acid or 500 nM inhibitor-2 mimicked the increases in I_{Ca} seen with calyculin A. These *in situ* studies identify constitutive activity of PP1 and the counteracting activity of certain isoforms of PKC, in pathways distinct from receptor-mediated signalling cascades, as regulatory components that determine the steady-state level of cardiac L-type I_{Ca}.

(Resubmitted 19 December 2003; accepted after revision 21 January 2004; first published online 23 January 2004)
Corresponding author W. H. duBell: Department of Biochemistry and Molecular Biology, University of Maryland School of Medicine, Baltimore, MD 21201, USA. Email: wdubell@som.umaryland.edu

Excitation–contraction coupling in cardiac cells is initiated by openings of L-type Ca^{2+} channels, which increases the local $[Ca^{2+}]_i$ that activates nearby sarcoplasmic reticulum Ca^{2+} release channels, or ryanodine receptors (Fabiato, 1983). The activation of a large number of ryanodine receptors gives rise to the $[Ca^{2+}]_i$ transient that activates contraction (Cheng *et al.* 1993). Excitation–contraction coupling is regulated by receptor-activated signalling pathways that frequently alter the phosphorylation state of Ca^{2+} handling proteins (Tada & Katz, 1982; Hartzell, 1988). It has been established that the action of kinases is integrated with protein phosphatase activity in these signalling pathways. For example, during the course of the cAMP–PKA cascade the serine/threonine phosphatase PP1 is inhibited (Ahmad *et al.* 1989; Gupta *et al.* 1996), augmenting the cAMP signal, while the Ca^{2+}-dependent phosphatase calcineurin is activated, perhaps limiting the action of PKA (Santana *et al.* 2002). The functional importance of phosphatases is underscored by observations from immunoprecipitation studies revealing

 DOI: 10.1113/jphysiol.2003.059329

that another phosphatase, PP2A, is bound to the RyR (Marx *et al.* 2001) and the α1-subunit of the L-type Ca^{2+} channel (Davare *et al.* 2000).

Several lines of evidence have established that even in the absence of humoral stimulation there is a dynamic balance between kinase and phosphatase activity that controls ventricular myocyte function. Our laboratory has shown that intracellular dialysis of rat ventricular myocytes with exogenous PP2A decreases the $[Ca^{2+}]_i$ transient and steady-state L-type I_{Ca} (duBell *et al.* 1996). Application of PP1/PP2A inhibitors such as okadaic acid can activate L-type Ca^{2+} channels both in intact myocytes (Hescheler *et al.* 1988; Neumann *et al.* 1993; Hirayama & Hartzell, 1997) and in cell-attached patches (Ono & Fozzard, 1993; Wiechen *et al.* 1995). Recently, we have shown that the phosphatase inhibitor calyculin A increases contractility in isolated mouse ventricular myocytes by increasing L-type Ca^{2+} channel activity (duBell *et al.* 2002). These studies reveal that there is an 'I_{Ca} reserve' that is maintained by this dynamic phosphorylation–dephosphorylation balance. The functional importance of this balance is seen in ventricular myocytes from failing human heart in which a blunted response to β-adrenergic agonists is accompanied by a loss in phosphatase-sensitive L-type Ca^{2+} channel reserve (Schröder *et al.* 1998; Chen *et al.* 2002).

The major goal of the present study was to identify the specific signalling enzymes that determine the set point, or basal level, of L-type I_{Ca}. This kinase–phosphatase balance was examined *in situ* in murine ventricular myocytes, a model system that is increasingly important due to the many transgenic mouse heart failure models that are available. The main findings are that PP1 is an important phosphatase in the steady-state regulation of L-type I_{Ca} and that the opposing kinase in this setting is neither PKA nor CaMKII, but rather one or more isoforms of PKC. The significance of these new results is seen in recent studies of both transgenic mouse lines and human myocardium that implicate PP1 in heart failure (Neumann *et al.* 1997; Carr *et al.* 2002).

Methods

Cardiac myocyte preparation

Ventricular myocytes were isolated from the hearts of adult male CD-1 mice. After deep anaesthesia was induced with 30 mg kg^{-1} (I.P.) sodium pentobarbital (Abbott Laboratories), the heart was removed and washed. The ascending aorta was rapidly cannulated for Langendorff perfusion. Following a brief period of perfusion with enzyme-free buffer, the heart was perfused with buffer containing Type 2 collagenase (Worthington Biochemical Corp.) and protease (Fraction XIV, Sigma Chemical Corp.) as previously described (duBell *et al.* 2000). Following the isolation procedure, the cells were maintained at room temperature in Hepes-buffered Dulbecco's modified Eagle's medium supplemented with heat-inactivated fetal calf serum (10%) and insulin (1 unit ml^{-1}). All experiments were carried out within 8 h of cell isolation

Voltage clamp and I_{Ca}

L-type Ca^{2+} currents were recorded at 35°C from single, isolated ventricular myocytes using low resistance (<1.5 MΩ) patch-type microelectrodes in the whole-cell mode. All experiments were conducted on a Nikon Diaphot 300 inverted microscope using an Axopatch 200A voltage-clamp amplifier with a CV202A headstage (Axon Instruments). Cells were placed in the experimental chamber and superfused with a solution containing 140 mM NaCl, 5 mM KCl, 10 mM Hepes, 1.0 mM $MgCl_2$, 0.33 mM NaH_2PO_4 and 10 mM D-glucose at pH 7.4 (NaOH). When Ca^{2+} currents were evoked from a holding potential of −40 mV (Figs 3–7), the cells were superfused with a similar solution with the exception that 5.0 mM CsCl replaced the KCl and 1.8 mM $CaCl_2$, 5 mM 4-aminopyridine (4-AP), 10 mM tetraethylammonium chloride (TEA) and 10 μM tetrodotoxin (TTX) were added. When Ca^{2+} currents were evoked from a holding potential of −80 mV (Figs 1 and 2), the extracellular solution was Na^+ and K^+ free and consisted of 150 mM TEACl, 5 mM CsCl, 10 mM Hepes, 1.0 mM $MgCl_2$, 10 mM dextrose, 1.8 mM $CaCl_2$, 5 mM 4-AP and 10 μM TTX. For all experiments, the pipette filling solution consisted of 120 mM CsCl, 15 mM TEACl, 5 mM MgATP, 10 mM Hepes, 1.0 mM $MgCl_2$ and 10 mM of either EGTA or BAPTA (pH to 7.2 with CsOH). The use of Cs^+, TEACl and 4-AP assured block of currents through K^+ channels and TTX was present to block currents through Na^+ channels.

The Ca^{2+} current recordings were low-pass filtered at 2 kHz by the voltage-clamp amplifier, digitized at 5 kHz (Digidata 1200, Axon Instruments) and stored on a computer for subsequent analysis. The current amplitudes were normalized to cell capacitance to account for differences in cell size and are reported as current densities (pA pF^{-1}). Cell capacitance was calculated by integrating the uncompensated capacity transients elicited by 10 ms hyperpolarizing pulses from −70 to −80 mV.

Calyculin A and staurosporine (Alexis) were prepared as 1 mM stocks in DMSO. H89 and Ro 31-8220 (Biomol) were prepared as 10 mM stocks in DMSO. Gö 6976 (Biomol)

was prepared as a 2 mM stock in DMSO. These stocks were added to the extracellular buffers to bring each agent to the indicated concentration. The control solutions included the same concentration of DMSO as the experimental solutions. The total extracellular concentration of DMSO never exceeded 0.04%. Okadaic acid (Alexis) was prepared as a 500 μM stock in DMSO and added to the filling solution. The final concentration of DMSO in the filling solution for each concentration of okadaic acid was 0.4%. Fostriecin (Alexis), 8-bromo cAMP (Calbiochem) and inhibitor-2 (Upstate Biotechnology) were prepared as aqueous stock solutions and added to the filling solution to the indicated concentrations.

Statistics

The experimental values are expressed as the means ± S.E.M. The sample size for each experiment is indicated in the figure legend or text, followed by the number of hearts from which those cells were taken. Statistical significance ($P < 0.05$) was assessed using either the paired or unpaired Student's t test, as appropriate.

Results

We have recently reported that the PP1/PP2A inhibitor calyculin A evokes a rapid and pronounced increase in the magnitudes of the mouse ventricular $[Ca^{2+}]_i$ transient and twitch contraction, responses that result principally from an increase in L-type I_{Ca} (duBell *et al.* 2002). In the present study, we extend these findings to characterize, *in situ*, the mechanisms of the dynamic control of the steady-state murine ventricular L-type Ca^{2+} current in the absence of humoral signalling.

Effects of calyculin A on the biophysical properties of the L-type Ca^{2+} current

Initial studies were performed to characterize the effects of calyculin A on the biophysical properties of macroscopic L-type I_{Ca}. In contrast to our previous study, which was carried out under conditions in which we could examine excitation–contraction coupling (duBell *et al.* 2002), the present experiments were performed with pipette filling solution containing 10 mM EGTA to minimize the effects of sarcoplasmic reticulum Ca^{2+} release on I_{Ca}. In addition, the initial experiments (Figs 1 and 2) were performed in the absence of internal and external Na^+ and K^+ to increase the voltage range over which I_{Ca} could be examined and to minimize overlapping inward and outward currents. It was not certain that calyculin A would increase I_{Ca} in the absence of intracellular Ca^{2+} transients, as we had previously seen in their presence (duBell *et al.* 2002). However, Fig. 1 shows that calyculin A did, in fact, increase I_{Ca} under these conditions. The magnitude of the current was significantly greater in calyculin A at all potentials between −42 and +49 mV (Fig. 1*B*). For example, the current at 0 mV increased from −12.0 ± 0.80 to −17.2 ± 1.2 pA pF^{-1} ($P = 0.001$). The increases at −7 and −14 mV were even greater because, in addition to increasing the amplitude of the current, calyculin A also shifted the peak of the I_{Ca}–voltage relationship in the hyperpolarizing direction, from 0 mV to −14 mV (Fig. 1*B*). This observation is emphasized in Fig. 2*A*, which shows the control and calyculin A I_{Ca}–voltage relationships normalized to the peak I_{Ca} observed in each experiment. Calyculin A exposure also resulted in an apparent shift in the voltage dependence of activation of I_{Ca}, with the threshold for activation of I_{Ca} shifting from −35 to −42 mV (control, 0.09 ± 0.06 pA pF^{-1}; calyculin A, −0.25 ± 0.04 pA pF^{-1}). However, calyculin A did not affect the kinetics of I_{Ca} decay. At 0 mV, the decay of the control current was well fitted by two exponentials with time constants (τ) of 22 ± 1 and 72 ± 2 ms. After calyculin A, the fast and slow time constants were 24 ± 1 ms ($P = 0.12$) and 82 ± 4 ms ($P = 0.07$), respectively. While the amplitude of the slow component remained unchanged following calyculin A (−4.77 ± 0.4 pA pF^{-1} in control *versus* −4.58 ± 0.6 with calyculin A, $P = 0.60$), the amplitude of the fast component was increased, from −7.7 ± 0.7 to −13.5 ± 0.8 pA pF^{-1} ($P = 0.0005$).

The effects of calyculin A on the voltage dependence of steady-state inactivation were also examined (Fig. 1*C* and *D*). At holding potentials between −90 and −48 mV, the current was significantly greater after calyculin A (−60 mV; control, 13.1 ± 1.0 pA pF^{-1}; calyculin A, 18.6 ± 1.2 pA pF^{-1}, $P = 0.0003$, Fig. 1*D*). However, at potentials between −27 and −13 mV, the current was significantly less after calyculin A (−60 mV; control, 3.61 ± 0.44 pA pF^{-1}; calyculin A, 2.72 ± 0.50 pA pF^{-1}, $P = 0.001$, Fig. 1*D*). These data suggest that in addition to its other effects, calyculin A shifted the voltage dependence of steady-state inactivation in the hyperpolarizing direction.

The data presented in Fig. 1 were used to construct normalized plots of both the voltage dependence of peak conductance (activation) and the voltage dependence of steady-state inactivation (Fig. 2*B*, see legend for details). Consistent with the hyperpolarizing shift in both the threshold for activation and the peak of the $I_{Ca}-V$ relationship, calyculin A also produced a hyperpolarizing shift in the voltage dependence of activation, with the

voltage at which activation was half-maximal ($V_{0.5}$) changing from −17 mV in control to −25 mV after calyculin A. As suggested by the data presented in Fig. 1*D*, the inactivation $V_{0.5}$ is also shifted in the hyperpolarizing direction, from a potential of −32 mV in control to −37 mV in calyculin A. Thus, these data reveal that a potent inhibitor of PP1/PP2A evokes fundamental changes in the macroscopic properties of murine ventricular whole-cell L-type Ca^{2+} current in the steady state.

Sequential addition of staurosporine and calyculin A

The large and rapid responses seen following application of calyculin A (Fig. 1) suggest that an active dynamic balance between phosphorylation (stimulation of I_{Ca}) and dephosphorylation (inhibition of I_{Ca}) determines the magnitude of the L-type Ca^{2+} current in the absence of any neurohumoral stimulation. In this scheme, the increase in I_{Ca} in response to calyculin A would result from kinase activity that becomes predominant following the inhibition of the counteracting phosphatase. Thus the notion that the action of calyculin A is dependent on kinase activity was tested through consecutive additions of calyculin A and the broad-spectrum kinase inhibitor staurosporine.

These experiments began with the recording of an I_{Ca}–voltage relationship under control conditions. The cells were then exposed to either calyculin A or staurosporine alone for 5 min. Following the recording of an I_{Ca}–voltage relationship in this condition, the cells were treated with

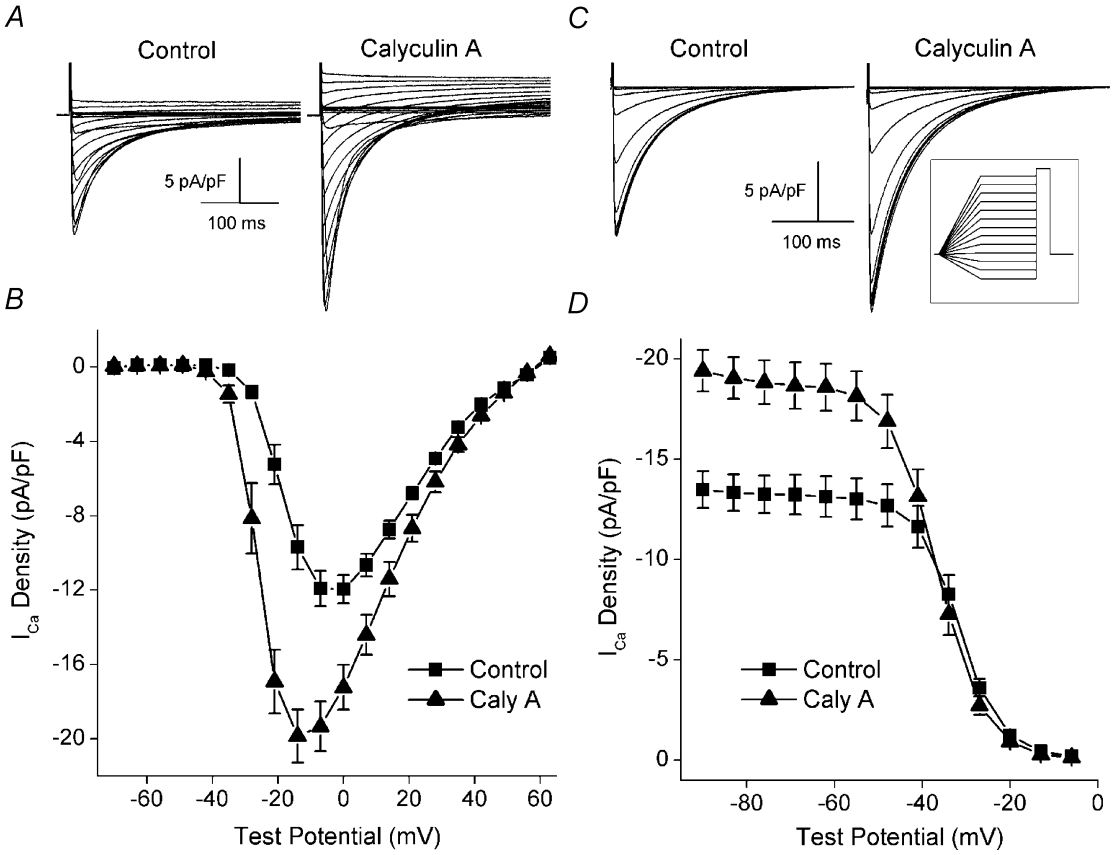

Figure 1. The effect of calyculin A on the voltage dependence and steady-state inactivation of I_{Ca}
A, L-type Ca^{2+} currents from the same cell before (left) and after (right) 5 min exposure to 100 nM calyculin A (Caly A). Internal and external solution were Na^+ and K^+ free. Test depolarizations (300 ms) were given to potentials between −70 and +63 mV from a holding potential of −80 mV. The interval between test pulses was 5 s. *B*, plots of the mean (± S.E.M., $n = 7, 3$) voltage dependence of I_{Ca} before (■) and after (▲) 5 min of exposure to 100 nM calyculin A. *C*, L-type Ca^{2+} currents from the same cell before (left) and after (right) 5 min of exposure to 100 nM calyculin A. Cells were held for 1200 ms at potentials between −90 and −6 mV following a 1000 ms ramp from −70 mV. I_{Ca} was elicited by a 300 ms test pulse to 0 mV, followed by repolarization to −70 mV, with an 8 s interval between test pulses (see inset for schematic). *D*, plots of mean (± S.E.M., $n = 8, 3$) I_{Ca} density *versus* holding potential before (■) and after (▲) 5 min of 100 nM calyculin A.

both calyculin A and staurosporine for an additional 5 min and another I_{Ca}–voltage relationship was recorded. These and all subsequent experiments were conducted in Na^+-containing solutions and the I_{Ca}–voltage relationships were determined from a holding potential of −40 mV to inactivate I_{Na} (see Methods and legend for Fig. 3). Control experiments (not shown) demonstrated that the effects of both calyculin A and staurosporine were complete within 5 min. In addition, control experiments in the absence of any inhibitors demonstrated that there was minimal I_{Ca} rundown over the same time period. For example, the magnitude of the current at 0 mV decreased by only about 5%, from −12.7 ± 1.7 to −12.0 ± 1.7 pA pF^{-1} ($n = 6$) and the decreases at other test potentials were comparably small. Figure 3*A* shows the results obtained when calyculin A was added first. After 5 min in calyculin A, there was a statistically significant increase in the magnitude of I_{Ca} at each test potential between −28 and +56 mV. For example, I_{Ca} increased by 33% from −13.9 ± 2.9 to −18.5 ± 2.9 pA pF^{-1} at 0 mV ($P = 0.0005$). In addition, calyculin A altered the voltage dependence of I_{Ca}, shifting the peak of the I_{Ca}–V relationship from 0 to −7 mV (Fig. 3*A*). Importantly, subsequent addition of staurosporine (300 nM) had no effect on the magnitude of I_{Ca} at any potential (−17.9 ± 3.3 pA pF^{-1} at 0 mV, $P = 0.20$). This latter experiment indicated that the kinase inhibitor alone did not display any significant non-specific effects on I_{Ca}.

In contrast, the results obtained when staurosporine was added first are quite different (Fig. 3*B*). Initial application of staurosporine had a marked effect on the magnitude of I_{Ca}, decreasing the current at all potentials between −21 and +56 mV. The current at 0 mV decreased by approximately 50%, from −11.8 ± 0.9 to −6.05 ± 0.42 pA pF^{-1}, after 5 min in staurosporine ($P = 0.0004$). Importantly, when calyculin A was added after staurosporine there was no increase in I_{Ca} at any potential, nor was there any shift in the voltage dependence of the current (Fig. 3*B*). These data support a model in which the amplitude of the steady-state L-type Ca^{2+} current is controlled by a balance between kinase and phosphatase activities, with the effects of calyculin A on I_{Ca} dependent on the stimulatory effects of the kinase and the effects of staurosporine dependent on the inhibitory effects of the phosphatase.

Calyculin A and protein kinase A inhibition

The effects of calyculin A on the macroscopic biophysical properties of the L-type Ca^{2+} current shown in Figs 1 and 2 are quite similar to those seen following stimulation of the β-adrenergic receptor–PKA cascade (Piacentino *et al.* 2000; Chen *et al.* 2002). Thus, it was intriguing to speculate that the increase in I_{Ca} evoked by calyculin A resulted from a shift in the kinase–phosphatase balance toward the activity of PKA. This hypothesis was further supported by the observation that 1 μM isoprenaline (isoproterenol) was without effect on I_{Ca} after 5 min exposure to 100 nM calyculin A (Fig. 4*A*).

Accordingly, the notion that PKA is involved in the steady-state regulation of murine ventricular L-type Ca^{2+}

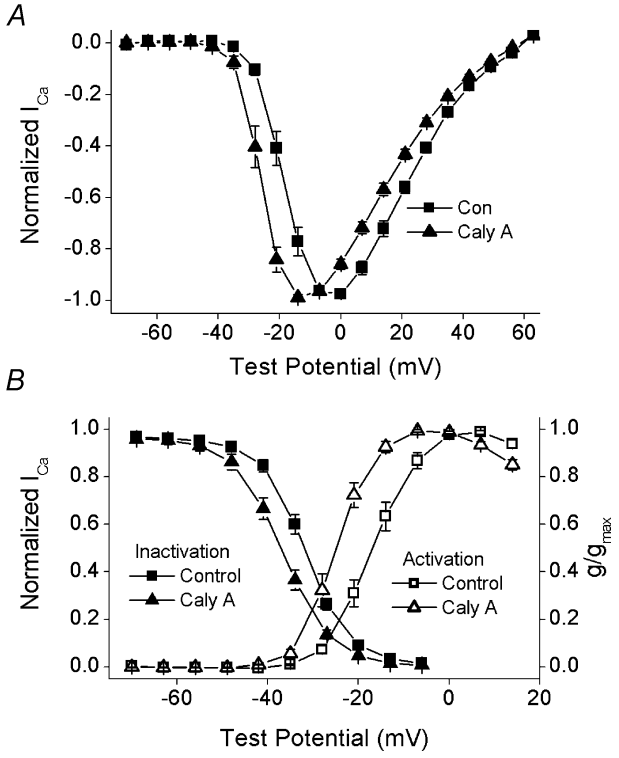

Figure 2. Effects of calyculin A on the voltage dependencies of activation and steady-state inactivation

A, normalized plots of the mean (± S.E.M., $n = 7$, 3) voltage dependence of I_{Ca} before (■) and after (▲) 5 min of exposure to 100 nM calyculin A. The current at each test potential was normalized to the maximum current from the experiment and the average values were plotted *versus* test potential. The plots are from the data used for Fig. 1*A* and *B*). Normalized plots of the voltage dependencies of activation (open symbols) and steady-state inactivation (filled symbols) from cells before (■, □) and after (▲, △) 100 nM calyculin A ($n = 8$, 3). Voltage dependence of activation was determined from the I_{Ca}–V relationships shown in Fig. 1*A*. The conductance (g) at each potential was calculated as $g = I_{Ca}/(E_m - E_{rev})$, where E_m is the test potential and E_{rev} the reversal potential, as determined from the I_{Ca}–V plot. The conductance was then normalized to the maximal conductance obtained during the experiment. Voltage dependence of steady-state inactivation was determined from data in Fig. 1*B*. The current at each holding potential was normalized to the largest current recorded during the experiment. The average values for each were plotted *versus* holding potential.

current was tested by using inhibitors of PKA. Rp-cAMPs, a competitive antagonist to cAMP, was used to block the activity of PKA (Rothermel & Parker-Botelho, 1988). Control experiments revealed that 100 μM Rp-cAMPs in the pipette filling solution completely blocked the effects of 100 nM isoprenaline on the I_{Ca}–voltage relationship (Fig. 4*B*). For example, the control value of I_{Ca} at 0 mV increased from -7.03 ± 0.9 to -16.6 ± 2.0 pA pF^{-1} in isoprenaline. However, when 100 μM Rp-cAMPs was included in the filling solution, isoprenaline failed to increase the amplitude of I_{Ca} at any potential (0 mV: -7.51 ± 0.8 pA pF^{-1} basal; -7.20 ± 0.8 pA pF^{-1} in the presence of isoprenaline). Unlike staurosporine (Fig. 3*B*), the cAMP-antagonist had no effect by itself on I_{Ca} density at any test potential (Fig. 4*C*). A comparison between 14 cells with and 10 cells without Rp-cAMPs revealed I_{Ca} densities of -9.2 ± 0.7 and 10.3 ± 1.2 pA pF^{-1}, respectively, at 0 mV ($P = 0.40$, unpaired t test) and a similar lack of effect at other test potentials (Fig. 4*C*). Furthermore, the stimulatory action of calyculin A was insensitive to this PKA-inhibitory dose of Rp-cAMPs (Fig. 4*C*). A subset of the cells dialysed with 100 μM Rp-cAMPs were exposed to calyculin A (see legend to Fig. 4). Under these conditions, calyculin A still increased I_{Ca} at all potentials between -21 and $+56$ mV. For example, I_{Ca} at 0 mV was increased by 60%, from -13.1 ± 1.4 to -20.9 pA pF^{-1} ($P = 0.006$).

It is important to note that Rp-cAMPs blocks PKA activation by inhibiting the cAMP-evoked dissociation of the regulatory subunit RII from the enzyme complex (Rothermel & Parker-Botelho, 1988). Although not likely, it is possible that a constitutively active, RII-free form of PKA could underlie the response to calyculin A. Accordingly, complementary experiments were performed with the PKA inhibitor H89, an established direct inhibitor, of the PKA catalytic subunit in ventricular myocytes (Yuan & Bers, 1994, 1995; You *et al.* 1997). As shown in Fig. 4*D*, cellular responses to H89 were nearly identical to those of Rp-cAMPs. For example, the average current densities at 0 mV in control and H89 were -12.9 ± 1.7 and -12.0 ± 1.9 pA pF^{-1}, respectively ($P = 0.27$). Further, I_{Ca} was significantly increased by calyculin A at all test potentials between -2 and $+56$ mV in H89-treated cells. At 0 mV,

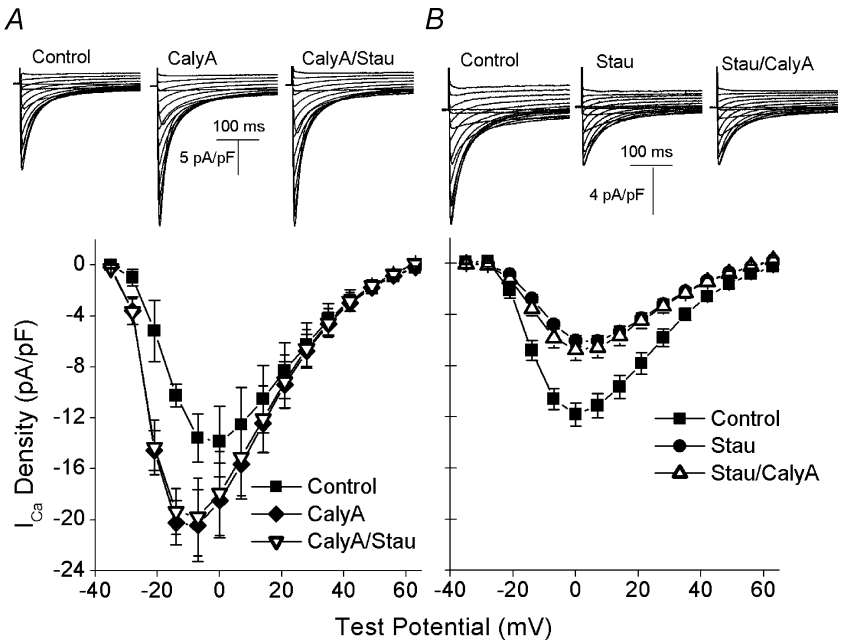

Figure 3. Effects of calyculin A and staurosporine on I_{Ca}–V relationship
A, top, L-type Ca^{2+} currents recorded from the same cell in control buffer (left), after 5 min in 100 nM calyculin A (centre) and after 5 min in 100 nM calyculin A and 300 nM staurosporine (right). The holding potential was -70 mV. After a 1000 ms voltage ramp to -40 mV, the cell was held at -40 mV for 330 ms and I_{Ca} was elicited by a 300 ms test pulse to a potential between -35 and $+60$ mV. There was a 5 s interval between each test pulse. *A*, bottom, superimposed plots of the mean (± S.E.M., $n = 4$, 2) voltage dependence of I_{Ca} in control (■), calyculin A (♦) and calyculin A–staurosporine (▽). *B*, top, L-type Ca^{2+} currents recorded from the same cell in control (left), after 5 min in 300 nM staurosporine (centre) and after 5 min in 300 nM staurosporine and 100 nM calyculin A (right). *B*, bottom, superimposed plots of the mean (± S.E.M., $n = 5$, 2) voltage dependence of I_{Ca} in control (■), staurosporine (●) and staurosporine–calyculin A (△).

the current was increased by 47%, from -9.49 ± 1.4 to -17.9 ± 2.6 pA pF^{-1} ($P = 0.036$). Taken together, these results eliminate PKA as the candidate kinase in the tonic regulation of I_{Ca}.

Calyculin A and CaMKII inhibition

Another kinase whose activity could be unmasked by calyculin A is the Ca^{2+}- and calmodulin-dependent protein kinase, CaMKII. Although the experiments in the present study were carried out under conditions of high Ca^{2+}-buffering, it has been shown that 10 mM EGTA does not buffer $[Ca^{2+}]_i$ sufficiently rapidly to prevent local increases in $[Ca^{2+}]_i$ and the subsequent activation of CaMKII (Naraghi & Neher, 1997; You *et al.* 1997). Thus, experiments were carried out using filling solution that contained 10 mM BAPTA. BAPTA is a more rapid buffer of Ca^{2+} (Naraghi & Neher, 1997; You *et al.* 1997) that has been shown to block CaMKII-dependent processes in ventricular myocytes (Xiao *et al.* 1994; Vinogradova *et al.* 2000). However, it is clear from the results presented in Fig. 5*A* that the calyculin A-evoked increases in I_{Ca} were completely insensitive to intracellular BAPTA (compare with Fig. 3). There was a significant increase in I_{Ca} at all potentials between -21 and $+49$ mV. The calyculin A-evoked increase at -7 mV was from -13.3 ± 1.9 to -24.4 ± 1.8 pA pF^{-1} ($P = 0.003$), comparable to the increase evoked by calyculin A in EGTA-treated cells (Fig. 3), from a control value of -13.6 ± 1.9 to -20.4 ± 2.8 pA pF^{-1} in calyculin A. To address the possibility that inclusion of 10 mM BAPTA still provided insufficient buffering to prevent local Ca^{2+}-dependent activation of CaMKII proximate to the channel, a series of complementary experiments was performed in which 1.8 mM Ba^{2+} was substituted for Ca^{2+} as the charge carrier. While Ba^{2+} is widely used as the permeant ion in studies of the L-type

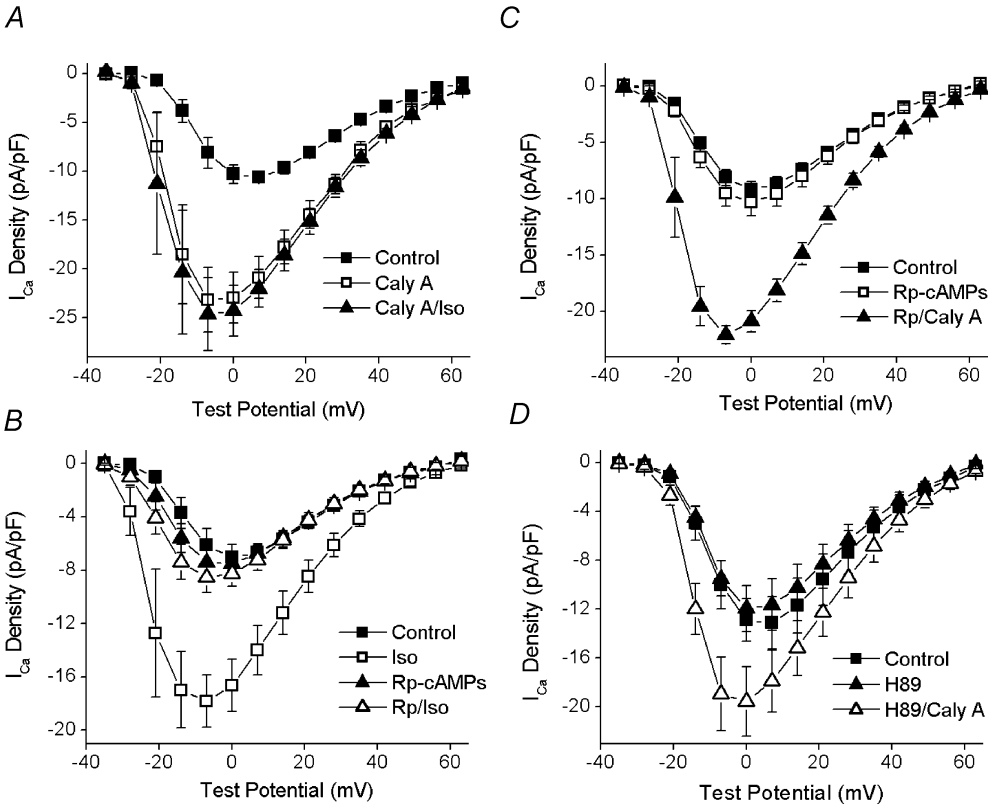

Figure 4. The effect of PKA inhibition on the response to calyculin A
A, I_{Ca}–*V* plots from control (■), after 5 min in 100 nM calyculin A (□) and after 5 min in 1 μM isoprenaline and 100 nM calyculin A (▲, $n = 4$, 2). *B*, I_{Ca}–*V* plots from control cells before (■) and after (□) 100 nM isoprenaline ($n = 4$, 2) and from cells dialysed with 100 μM Rp-cAMPs before (▲) and after (△) isoprenaline ($n = 5$, 3). *C*, I_{Ca}–*V* plots from control cells (■; $n = 14$, 7), cells dialysed with 100 μM Rp-cAMPs (□; $n = 10$, 4) and a subset of the cells dialysed with 100 μM Rp-cAMPs that were subsequently superfused with 100 nM calyculin A (▲; $n = 5$, 2). *D*, I_{Ca}–*V* plots in control (■), after 5 min in 1 μM H89 (▲) and after 5 min in H89 and 100 nM calyculin A (△) ($n = 4$, 3).

Ca^{2+} channel (Ono & Fozzard, 1993; Xiao *et al.* 1994; Wiechen *et al.* 1995; Wu *et al.* 1999; Dzhura *et al.* 2000), this ion cannot activate CaMKII (Chao *et al.* 1984). As shown in Fig. 5*B*, L-type Ca^{2+} channel-mediated Ba^{2+} currents were still increased by calyculin A and the peak of the I_{Ca}–V relationship was shifted in the hyperpolarizing direction. Taken together, these data indicate that CaMKII activity is not responsible for the activation of I_{Ca} observed following phosphatase inhibition with calyculin A.

Calyculin A and PKC inhibition

Several studies have implicated PKC in receptor-mediated regulation of the L-type Ca^{2+} channel (for review see Kamp & Hell, 2000). Accordingly, it was a priority to assess the role of PKC in the action of calyculin A on I_{Ca}. The pan-specific PKC inhibitor Ro 31-8220 was used for this purpose. As shown in Fig. 6*A*, Ro 31-8220 had no effect on calyculin A-stimulated I_{Ca}. However, when Ro 31-8220 was applied before calyculin A, the results were quite different. Ro 31-8220 decreased the amplitude of I_{Ca} at each potential between −14 and +49 mV. For example, the current density at 0 mV decreased from -12.6 ± 1.2 to -8.5 ± 0.50 pA pF^{-1} ($P = 0.006$, see Fig. 6*A*). Following Ro 31-8220, calyculin A significantly increased I_{Ca} at all potentials between −28 and +49 mV. However, the response was significantly attenuated, as I_{Ca} increased only to the initial control values (Fig. 6*A*). These results suggest the possibility that PKC is involved in the determination of the basal level of I_{Ca} in these cells. This idea was tested further in studies with another inhibitor, Gö 6976. The effects of Gö 6976 were similar to those of Ro 31-8220 (Fig. 6*B*). Gö 6976 decreased the current only when added before calyculin A, and prior exposure to this inhibitor blunted the response of I_{Ca} to calyculin A. For example, the average current at 0 mV when calyculin A was added after Gö 6976 was -11.6 ± 1.2 pA pF^{-1}, identical to the control value of -11.9 ± 0.78 pA pF^{-1}. It is important to note that, of the specific kinase inhibitors utilized in the present study, only the PKC inhibitors decreased the amplitude of basal I_{Ca} and attenuated the calyculin A-induced activation of I_{Ca}.

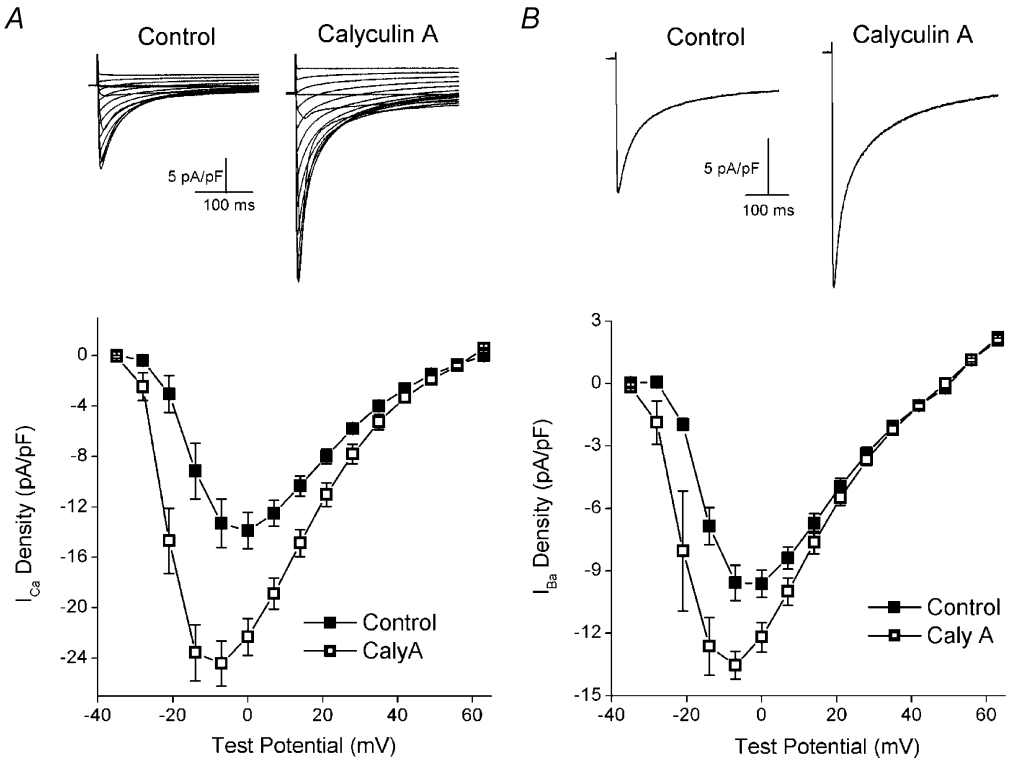

Figure 5. Effects of minimizing CaMKII activity on the response to calyculin A
A, top, currents recorded before (left) and after (right) exposure to 100 nM calyculin A using pipette filling solution containing 10 mM BAPTA. *A*, bottom, mean (± S.E.M., $n = 5$, 2) I_{Ca}–V relationships before (■) and after (□) 100 nM calyculin A. *B*, top, representative currents elicited by steps to 0 mV with 1.8 mM Ba^{2+}, instead of Ca^{2+}, as the charge carrier. *B*, bottom, mean (± S.E.M., $n = 4$, 1) current–voltage relationships from these experiments before (■) and after (□) 100 nM calyculin A.

Potential non-specific effects of PKC inhibitors are a concern. However, since neither Gö 6976 nor Ro 31-8220 had any effect on I_{Ca} in calyculin A-treated cells, direct effects on the channel are unlikely. In addition, β-adrenergic stimulation has been reported to result in activation of PKC (Yabe *et al.* 1998) so it is possible that the effects of the PKC inhibitors may result from an interaction with the PKA pathway. Thus, a series of control experiments were carried out to examine this possibility by comparing the ability of isoprenaline to increase I_{Ca} in the absence and presence of 1 μM Ro 31-8220. In control cells, there was little change over 5 min in I_{Ca} at any potential. The values at 0 mV were -12.9 ± 1.3 and -11.4 ± 0.7 pA pF^{-1} after 5 min ($n = 3, 3$; $P = 0.12$). After 5 min in 100 nM isoprenaline, I_{Ca} at 0 mV reached -21.8 ± 2.5 pA pF^{-1}. As was seen in Fig. 6*A*, 5 min exposure to 1 μM Ro 31-8220 decreased I_{Ca} at all potentials. In this sample ($n = 6, 5$), I_{Ca} at 0 mV decreased from -12.5 ± 0.7 to -9.2 ± 0.6 pA pF^{-1} ($P = 0.001$). Following Ro 31-8220, isoprenaline increased I_{Ca} at all potentials, with the average at 0 mV reaching -19.4 ± 1.9 pA pF^{-1}. The amplitude of I_{Ca} after isoprenaline in the presence of Ro 31-8220 was statistically indistinguishable from its amplitude after isoprenaline in control cells ($P = 0.46$ at 0 mV, unpaired t test). These observations support the view that the effects of PKC inhibitors in the present study result only from PKC inhibition. Thus, along with the results shown in Fig. 6, they are consistent with the view that at least one, and possibly more, isoforms of PKC are involved in the tonic regulation of I_{Ca}.

The effects of specific PP1 and PP2A inhibitors

An important goal of this study was to identify the specific phosphatase that controls steady-state I_{Ca} activity *in situ*. We have previously demonstrated that calyculin A blocks both PP1 and PP2A under the conditions used in the present study (duBell *et al.* 2002). Okadaic acid also inhibits both PP1 and PP2A but it has a dose–inhibition profile that allows for a distinction between the activities of these two enzymes (Bialojan & Takai, 1988). Accordingly, okadaic acid was dialysed into cells as a component of the pipette filling solution at concentrations of 10 nM, 100 nM and 2 μM (Fig. 7*A*). Note that the I_{Ca}–V plots for both 10

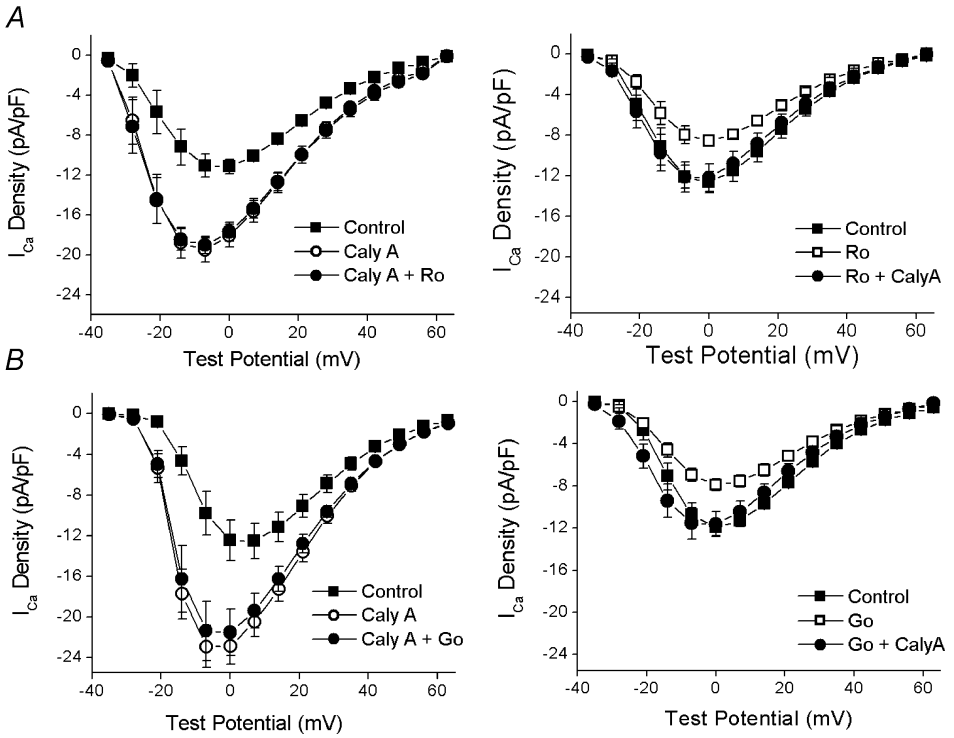

Figure 6. The effects of PKC inhibition with Ro 31-8220 and Gö 6976 on the response to calyculin A
A, left, superimposed plots of the voltage dependence of I_{Ca} in control (■), after 5 min in 100 nM calyculin A (○) and after 5 min in calyculin A and 1 μM Ro 31-8220 (●, $n = 6, 2$). *A*, right, similar panel with the reverse order of application ($n = 8, 4$): Control (■), 1 μM Ro 31-8220 (□) and Ro 31-8220 and 100 nM calyculin A (●). *B*, left, voltage dependence of I_{Ca} in control (■), after 5 min in 100 nM calyculin A (○) and after 5 min in calyculin A and 200 nM Gö 6976 (●, $n = 5, 2$). *B*, right, similar panel with the reverse order of application ($n = 9, 2$): Control (■); 200 nM Gö 6976 (□) and Gö 6976 and 100 nM calyculin A (●).

and 100 nM okadaic acid superimpose and that the peak of each is at 0 mV. The current densities at 0 mV were -13.6 ± 2.06 and -13.8 ± 0.9 pA pF^{-1} with 10 and 100 nM okadaic acid, respectively ($P = 0.95$, unpaired t test). Further, these values are very close to the established control values. This is emphasized in Fig. 7*C*, a histogram showing the average effects on I_{Ca} at 0 mV of the phosphatase inhibitors used in the present study. When the pipette solution contained 2 μM okadaic acid, however, there was a marked increase in I_{Ca} density. For example, the average current density at 0 mV was -21.2 ± 1.9 pA pF^{-1} ($P = 0.015$, unpaired t test, compared to 10 nM okadaic acid). In addition, the increase in I_{Ca} was accompanied by the characteristic shift in the peak of the I_{Ca}–V relationship from 0 to -7 mV (Fig. 7*A*). These data suggest that PP1, rather than PP2A, is important in the tonic regulation of I_{Ca}.

This hypothesis was further explored in more precise experiments using fostriecin and inhibitor-2, specific inhibitors of PP2A and PP1, respectively. When fostriecin (Walsh *et al.* 1997) was included in the pipette at 500 nM, there was no change in either the amplitude of I_{Ca} (Fig. 7*C* and 0 mV, control, -11.6 ± 0.85 pA pF^{-1} ($n = 6, 2$); fostriecin, -11.9 ± 1.8 pA pF^{-1} ($n = 5, 2$), $P = 0.85$, unpaired t test) or on the peak of the I_{Ca}–V relationship (data not shown). However, as shown in Fig. 7*B*, a calyculin A-like effect was indeed observed in the cells dialysed with 500 nM inhibitor-2, a specific protein inhibitor of PP1 (Silberman *et al.* 1984). Note that in the presence of inhibitor-2, the current density was significantly increased at all potentials between -21 and $+14$ mV ($P < 0.05$, unpaired t tests) and that the characteristic leftward shift, from 0 to -7 mV, was observed in the peak of the I_{Ca}–V relationship. Thus, the data presented in Fig. 7 reveal that PP1, and not PP2A, is an important regulator of the steady-state L-type Ca^{2+} current in intact cardiac myocytes.

Discussion

Since L-type Ca^{2+} channels play a central role in Ca^{2+} homeostasis in cardiac cells, neurohumoral regulation of I_{Ca} through kinases and phosphatases has been the subject of study in several laboratories (Hartzell, 1988; Trautwein & Hescheler, 1990; Kamp & Hell, 2000; Herzig & Neumann, 2000). Studies of signal transduction pathways

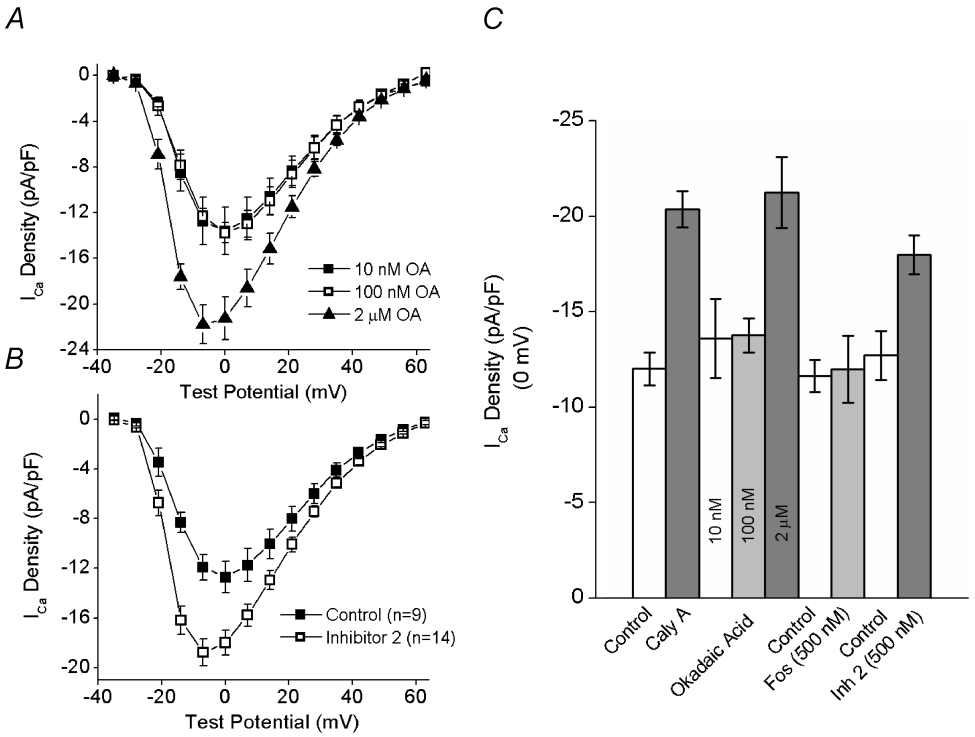

Figure 7. Effects of intracellular okadaic acid and inhibitor–2 on the I_{Ca}–V relationship
A, mean (± S.E.M.) I_{Ca}–V plots from cells dialysed with okadaic acid (OA) in concentrations of 10 nM (■; $n = 5$, 2), 100 nM (□; $n = 4$, 2) and 2 μM ▲; $n = 6$, 2). *B*, average I_{Ca}–V plots from control cells (■; $n = 9$, 4) and cells dialysed with 500 nM inhibitor-2 (□; $n = 11$, 6). *C*, summary histogram of the effects of calyculin A, okadaic acid, fostriecin and inhibitor-2 at 0 mV. The first two bars represent the average I_{Ca} before and after calyculin A from all of the experiments in which calyculin A was added in the absence of any inhibitors ($n = 19$, 8; data from Figs 3*A*, 4*A* and 6*A* and *B*).

have revealed that active modulation of Ca^{2+} influx through I_{Ca} results from a coordinated interplay in the activities of kinases and phosphatases. For example, in the well-known β-adrenergic receptor–PKA cascade, inhibitor-1 is a downstream PKA target, and is activated to attenuate PP1 activity (Ahmad *et al.* 1989; Gupta *et al.* 1996). Recently, Santana *et al.* (2002) provided evidence that the phosphatase calcineurin opposes the action of PKA in mouse ventricular myocytes, providing a Ca^{2+}-dependent mechanism for limiting the action of β-agonists. However it is not clear at present how these two distinct phosphatase pathways integrate to regulate I_{Ca} during the PKA cascade.

Other data demonstrate a regulatory model in which I_{Ca} is precisely modulated by a dynamic kinase–phosphatase balance even in the absence of humoral stimulation. For example, application of serine/threonine phosphatase inhibitors alone is sufficient to increase whole-cell I_{Ca} in frog (Frace & Hartzell, 1993), guinea-pig (Hescheler *et al.* 1987, 1988; Neumann *et al.* 1993, 1994; Hirayama & Hartzell, 1997), and more recently mouse ventricular myocytes (duBell *et al.* 2002). In a complementary study we have shown that addition of exogenous protein phosphatase 2A decreased I_{Ca} in rat ventricular myocytes (duBell *et al.* 1996). While the molecular details of this dynamic signalling system remain to be defined, the critical importance of this constitutive kinase–phosphatase balance in human heart disease was recently illuminated by studies on myocytes from failing human hearts. Defective Ca^{2+} homeostasis in cells from failing hearts results in part from a disruption of kinase–phosphatase control of I_{Ca}, as phosphatase inhibitors fail to increase I_{Ca} in the normal manner (Schröder *et al.* 1998; Chen *et al.* 2002). These studies suggest that a loss of 'I_{Ca} reserve', whereby the ability of I_{Ca} to increase in response to physiological demand is severely limited, may be a central feature of human heart failure. Thus, it is important to identify the molecular details of the kinase–phosphatase balance responsible for the tonic regulation of I_{Ca} in cardiac myocytes.

The goal of the present study was to identify signalling enzymes that control 'basal' cardiac L-type Ca^{2+} channel activity *in situ*. We examined this issue in mouse ventricular myocytes because of the growing importance of murine models in the study of heart disease. Further, we recently reported that increased twitch contraction in such cells after exposure to the PP1/PP2A inhibitor calyculin A was entirely attributable to increased L-type I_{Ca} (duBell *et al.* 2002). A finding reported here is that PP1 is an important modulator of steady-state I_{Ca}. Another conclusion is that the opposing kinase, rather than PKA or CaMKII, is probably one or more members of the protein kinase C family. Importantly, these studies provide new insights into the local control of I_{Ca} and illuminate the distinction between the pathways that underlie the tonic regulation of I_{Ca} and those that modulate I_{Ca} in response to receptor-activated signalling pathways.

Throughout the studies reported here there is a consistent, unifying pattern to the results that allowed an *in situ* analysis of the dynamic integration of phosphatase–kinase signalling. First, basal, steady-state, Ca^{2+} current levels were in the region of -12 pA pF^{-1} under the conditions used (see Figs 3–7). Second, serine/threonine phosphatase inhibitors, when effective, acted only to increase basal I_{Ca} to the -18 to -21 pA pF^{-1} range (see Figs 3–7). Third, protein kinase inhibitors, when effective, displayed two clear, reproducible effects. When applied first they reduced the basal, steady-state Ca^{2+} current levels to the 6–8 pA pF^{-1} range (Figs 3*B* and 6*A* and *B*) and they markedly limited the calyculin A-evoked increases to the 11–12 pA pF^{-1} range (Figs 3*B* and 6*A* and *B*) compared to control cells treated with calyculin A alone (21 pA pF^{-1}). Other experiments argued against a non-specific effect of the protein kinase inhibitors, as these agents had no effect on I_{Ca} in cells that were pretreated with calyculin A (Figs 3*A* and 6*A* and *B*). Thus, such striking reciprocity of action of kinase and phosphatase inhibitors on I_{Ca} allowed us to analyse the steady-state balance between kinases and phosphatases *in situ*.

PP1 *versus* PP2A

The use of broad spectrum serine/threonine phosphatase inhibitors has revealed the importance of dephosphorylation mechanisms in the control of L-type Ca^{2+} channels in normal and failing heart (Hescheler *et al.* 1987, 1988; Neumann *et al.* 1993, 1994; duBell *et al.* 1996; Hirayama & Hartzell, 1997; Schröder *et al.* 1998; Chen *et al.* 2002). Accordingly, an important goal in this study was to identify the phosphatase that contributes to the 'set point' or reserve of steady-state I_{Ca}. A variety of previous studies led us to suspect that PP2A was that phosphatase. First, we have shown that intracellular addition of exogenous PP2A decreases basal L-type I_{Ca} (duBell *et al.* 1996). Further, PP2A is bound constitutively to the α_{1c} subunit of the L-type Ca^{2+} channel. In brain, this phosphatase is part of the L-type Ca^{2+} channel macromolecular signalling complex and reverses the effects of PKA (Davare *et al.* 2000, 2001). Finally, we have previously shown that calyculin A is a powerful PP2A inhibitor under the conditions used here

(duBell *et al.* 2002). However, our results (Fig. 7) show that low concentrations of okadaic acid (10 and 100 nM), conditions that inhibit PP2A and not PP1 (Bialojan & Takai, 1988), and the selective PP2A inhibitor fostriecin (Walsh *et al.* 1997) are without effect on I_{Ca}. Rather, several results presented here reveal that PP1 is important in this regulation. First, okadaic acid increased I_{Ca} only at concentrations within the range that inhibits PP1 (Bialojan & Takai, 1988). In addition, more precise studies showed that inhibitor-2, a selective protein inhibitor of PP1 (Silberman *et al.* 1984), also markedly increased I_{Ca}. These results provide evidence that PP1 is important in controlling steady-state L-type Ca^{2+} channel activity. They are consistent with cell-attached patch-clamp studies of L-type Ca^{2+} channels conducting Ba^{2+} currents which suggest that PP-1 inhibition results in increased ion flux through single L-type Ca^{2+} channels (Ono & Fozzard, 1993; Wiechen *et al.* 1995). Taken together, our results indicate the importance of PP1, and little or no role for PP2A, in determining the level of I_{Ca} in the absence of receptor-mediated signalling.

There is an apparent inconsistency with our previous studies which showed that PP2A, and not PP1, inhibited basal I_{Ca} (duBell *et al.* 1996). However in this earlier study the role of phosphatases was studied by adding excess exogenous enzymes in the pipette filling solution. In contrast, the present experiments critically examine the role of endogenous phosphatases *in situ*, including locally targeted forms.

PKA

Several lines of evidence strongly implicated PKA as the counter-acting kinase that regulated I_{Ca}. First, it is well established that PKA stimulates ventricular I_{Ca} (Hartzell, 1988; Trautwein & Hescheler, 1990; Kamp & Hell, 2000) and recent work has shown that PKA is part of the L-type Ca^{2+} channel complex (Davare *et al.* 1999, 2001) through interactions with AKAPs (Gao *et al.* 1997; Davare *et al.* 1999). Further, the electrophysiological analysis reported here strongly implicated this kinase in mouse ventricle. In particular, calyculin A produced a hyperpolarizing shift in the voltage dependence of I_{Ca}, as well as the activation and steady-state inactivation curves; effects similar to those reported by others for β-adrenergic stimulation (Piacentino *et al.* 2000; Chen *et al.* 2002). Also, isoprenaline was without effect when added following calyculin A (Fig. 4*A*).

Thus, studies that critically examined the importance of PKA were warranted. Accordingly, inhibitors were used that would either prevent the cAMP-induced activation of PKA (Rp-cAMPs, Fig. 4*B* and *C*) or directly inhibit its activity (H89, Fig. 4*D*). Our experiments demonstrated that both of these agents failed to alter either the amplitude of steady-state I_{Ca} or the calyculin A-induced increase of I_{Ca}. A recent report by Santana *et al.* (2002) has suggested that PKA regulates basal I_{Ca} in mouse ventricular myocytes. However, as this was deduced primarily from an H89-dependent decrease in contraction, it is not clear if H89 decreased I_{Ca}. In contrast, others report that PKA inhibition has no effect on mammalian ventricular I_{Ca}. For example, Hirayama & Hartzell (1997) showed that intracellular dialysis with 2 mM Rp-cAMPs failed to decrease guinea-pig ventricular I_{Ca}, and more recently Chen *et al.* (2002) reported that H89 has no effect on I_{Ca} in human ventricular myocytes. Thus, the results presented here combined with those of others (Hirayama & Hartzell, 1997; Chen *et al.* 2002) support the view that constitutive PKA is not important in maintaining steady-state mammalian ventricular I_{Ca}. However, the case may be different in atrial cells, as Wang & Lipsius (1995) showed that basal I_{Ca} in feline atrial cells was decreased by both Rp-cAMPs and H89, implicating the importance of cAMP-PKA cascade in these cells in the absence of external signalling.

CaMKII

CaMKII was another protein kinase that required consideration. Blitzer *et al.* (1998) have shown in brain that inhibition of PP1 is linked to the activation of CaMKII. In heart, CaMKII not only colocalizes with L-type Ca^{2+} channels (Wu *et al.* 1999; Vinogradova *et al.* 2000) but activation of the kinase by flash photolysis of caged Ca^{2+} increases I_{Ca} as well (Anderson *et al.* 1994). Further, stimulation-dependent facilitation of I_{Ca} has been attributed to CaMKII activity (Yuan & Bers, 1994; Xiao *et al.* 1994; Dzhura *et al.* 2000).

Our initial strategy was to assess the importance of CaMKII using the rapid Ca^{2+} chelator BAPTA. While EGTA can effectively buffer global $[Ca^{2+}]_i$, it is not a sufficiently rapid buffer to prevent accumulation of local Ca^{2+} at the mouth of the channel during Ca^{2+} influx (Naraghi & Neher, 1997; You *et al.* 1997). In contrast, BAPTA, with its rapid Ca^{2+} binding kinetics, is a more useful buffer for preventing an increase in local $[Ca^{2+}]_i$ (Naraghi & Neher, 1997; You *et al.* 1997). Thus, CaMKII-dependent facilitation of rat ventricular I_{Ca} is blocked by 10 mM intracellular BAPTA but not by 10 mM EGTA (Xiao *et al.* 1994) and BAPTA blocks the CaMKII-mediated effects on I_{Ca} inactivation and reactivation that promote pacemaker activity in sinoatrial-nodal cells (Vinogradova

et al. 2000). In a second, independent approach, Ba^{2+} was used as the charge carrier. While Ba^{2+} can freely permeate through the L-type Ca^{2+} channel, it cannot activate calmodulin and CaMKII (Chao *et al.* 1984). Like BAPTA, it has been shown to prevent CaMKII-dependent regulation of the L-type Ca^{2+} current (Xiao *et al.* 1994; Dzhura *et al.* 2000). Nonetheless, neither intracellular BAPTA nor Ba^{2+} blocked the increase in current through the L-type Ca^{2+} channels in response to calyculin A. While the increase in I_{Ca} elicited by calyculin A in the presence of BAPTA is comparable to that seen with EGTA (compare Fig. 5*A* to Figs 3*A* and 6*A* and *B*), it appears as if the effect of calyculin A on Ba^{2+} currents is reduced. However, this is likely to be the result of the reduced ion-dependent inactivation that characterizes Ba^{2+} currents through L-type Ca^{2+} channels (Dzhura *et al.* 2000) and the fact that current amplitude was calculated as the difference between the peak inward current and the current remaining at the end of the voltage-clamp pulse. Thus, although CaMKII has been linked to Ca^{2+} channel regulation in several settings, the combined results of the BAPTA and Ba^{2+} experiments exclude a role for CaMKII in the regulation of the steady-state level of I_{Ca}.

PKC

The role for PKC in regulating cardiac I_{Ca} has been the subject of much investigation, with different effects of PKC activation reported for different species and for different PKC-activating agonists (Kamp & Hell, 2000). It is likely that some of these differences arise from the large number of different isoforms of PKC that exist within cardiac cells as well as from the method of activation of PKC. In the present study, we considered the possibility of a constitutively active PKC, presumably localized near the L-type Ca^{2+} channel, which is part of the kinase–phosphatase balance that we have observed. It is interesting to note that Tseng & Boyden (1991) found that activation of PKC increased I_{Ca} and left-shifted both activation and steady-state inactivation in canine ventricular myocytes and Purkinje cells, similar to the effect that we observe when background kinase activity is unmasked by inhibition of PP1 with calyculin A (Fig. 3) or inhibitor-2 (Fig. 7). A role for PKC in the steady-state regulation of mouse ventricular L-type Ca current was further supported by our results with two distinct PKC inhibitors, Ro 31-8220 and Gö 6976. Both of these inhibitors were effective in blocking the action of calyculin A on I_{Ca} (Fig. 6). Although non-specific effects of PKC inhibitors on I_{Ca} have been reported (Hartzell & Rinderknecht, 1996), neither Ro 31-8220 nor Gö 6976 had any effect on I_{Ca} when added after calyculin A, arguing against any such non-specific actions of these compounds. In addition, Ro 31-8220 did not modulate the effects of β-adrenergic stimulation, further arguing against any non-specific interactions.

Thus, the results reported in the present study illuminate an I_{Ca}-activating pathway for PKC in heart. While these results might seem to be in contrast to recent reports identifying an inhibitory role for PKC on L-type current (McHugh *et al.* 2000; Hu *et al.* 2000), there are many different forms of PKC and it is likely that distinct isozymes of PKC act at different sites and have opposing regulatory effects on the L-type Ca^{2+} channel. For example, phorbol esters inhibit I_{Ca} in TSA-201 cells expressing the recombinant rabbit cardiac a_{1c} subunit (McHugh *et al.* 2000), yet these agents increase the current when the same protein is expressed in *Xenopus* oocytes (Shistik *et al.* 1998). Recent studies link PKCϵ activation with inhibition of I_{Ca} in heart cells (Hu *et al.* 2000; Mochly Rosen *et al.* 2000) and Thr27 and Thr31 of the a_{1c} subunit may be the targets of PKC in this pathway (McHugh *et al.* 2000). However, there are also many reports that reveal a PKC-dependent pathway that increases L-type I_{Ca} in heart (Tseng & Boyden, 1991; Kelso *et al.* 1996; Woo & Lee, 1999; Kurata *et al.* 1999; He *et al.* 2000). It is important to note that because our experimental protocols do not involve the direct activation of PKC, the results of these experiments cannot be interpreted to either agree or disagree with the reports cited above. Rather, our present results support the view that one or more isoforms of PKC exerts tonic, positive control of ventricular L-type I_{Ca}. However, the identification of the underlying PKC species and its molecular substrate(s) requires further study.

In summary, the results of the present study support the view that PP1 and an isoform of PKC counteract one another to determine the set-point of the mouse ventricular L-type Ca^{2+} current. It will be important to determine how this system, which maintains a functional reserve of I_{Ca}, is altered in failing heart. A thorough understanding of this regulatory pathway, which is distinct from receptor-activated signalling, may lead to new clinical options for the enhancement of contractility.

References

Ahmad Z, Green FJ, Subuhi HS & Watanabe AM (1989). Autonomic regulation of type 1 protein phosphatase in cardiac muscle. *J Biol Chem* **264**, 3859–3863.

Anderson ME, Braun AP, Schulman H & Premack BA (1994). Multifunctional Ca^{2+}/calmodulin-dependent protein kinase mediates Ca^{2+}-induced enhancement of the L-type Ca^{2+} current in rabbit ventricular myocytes. *Circ Res* **75**, 854–861.

Bialojan C & Takai A (1988). Inhibitory effect of a marine-sponge toxin, okadaic acid, on protein phosphatases. Specificity and kinetics. *Biochem J* **256**, 283–290.

Blitzer RD, Connor JH, Brown GP, Wong T, Shenolikar S, Iyengar R & Landau EM (1998). Gating of CaMKII by cAMP-regulated protein phosphatase activity during LTP. *Science* **280**, 1940–1943.

Carr AN, Schmidt AG, Suzuki Y, del Monte F, Sato Y, Lanner C, Breeden K, Jing S-L, Allen PB, Greengard P, Yatani A, Hoit BD, Grupp IL, Hajjar RJ, DePaoli-Roach AA & Kranias EG (2002). Type 1 phosphatase, a negative regulator of cardiac function. *Mol Cell Biol* **22**, 4124–4135.

Chao SH, Suzuki Y, Zysk JR & Cheung WY (1984). Activation of calmodulin by various metal cations as a function of ionic radius. *Mol Pharmacol* **26**, 75–82.

Chen X, Piacentino III V, Furukawa S, Goldman B, Margulies KB & Houser SR (2002). L-Type Ca^{2+} channel density and regulation are altered in failing human ventricular myocytes and recover after support with mechanical assist devices. *Circ Res* **91**, 517–524.

Cheng H, Lederer WJ & Cannell MB (1993). Calcium sparks: elementary events underlying excitation-contraction coupling in heart muscle. *Science* **262**, 740–744.

Davare MA, Avdonin V, Hall DD, Peden EM, Burette A, Weinberg RJ, Horne MC, Hoshi T & Hell JW (2001). A β_2 adrenergic receptor signaling complex assembled with the Ca^{2+} channel Ca_v 1.2. *Science* **293**, 98–101.

Davare MA, Dong F, Rubin CS & Hell JW (1999). The A-kinase anchor protein MAP2B and cAMP-dependent protein kinase are associated with class C L-type calcium channels in neurons. *J Biol Chem* **274**, 30280–30287.

Davare MA, Horne MC & Hell JW (2000). Protein phosphatase 2A is associated with class C L-type calcium channels (Ca_v1.2) and antagonizes channel phosphorylation by cAMP-dependent protein kinase. *J Biol Chem* **275**, 39710–39717.

duBell WH, Gigena MS, Guatimosim S, Long X, Lederer WJ & Rogers TB (2002). Effects of PP1/PP2A inhibitor calyculin A on the E-C coupling cascade in murine ventricular myocytes. *Am J Physiol Heart Circ Physiol* **282**, H38–H48.

duBell WH, Lederer WJ & Rogers TB (1996). Dynamic modulation of excitation-contraction coupling by protein phosphatases in rat ventricular myocytes. *J Physiol* **493**, 793–800.

duBell WH, Lederer WJ & Rogers TB (2000). K^+ currents responsible for repolarization in mouse ventricle and their modulation by FK-506 and rapamycin. *Am J Physiol Heart Circ Physiol* **278**, H886–H897.

Dzhura I, Wu Y, Colbran RJ, Balser JR & Anderson ME (2000). Calmodulin kinase determines calcium-dependent facilitation of L-type calcium channels. *Nature Cell Biol* **2**, 173–177.

Fabiato A (1983). Calcium-induced release of calcium from the cardiac sarcoplasmic reticulum. *Am J Physiol Cell Physiol* **245**, C1–C14.

Frace AM & Hartzell HC (1993). Opposite effects of phosphatase inhibitors on L-type calcium and delayed rectifier currents in frog cardiac myocytes. *J Physiol* **472**, 305–326.

Gao T, Yatani A, Dell'Acqua ML, Sako H, Green SA, Dascal N, Scott JD & Hosey MM (1997). cAMP-dependent regulation of cardiac L-type Ca^{2+} channels requires membrane targeting of PKA and phosphorylation of channel subunits. *Neuron* **19**, 185–196.

Gupta RC, Neumann J, Watanabe AM, Lesch M & Sabbah HN (1996). Evidence for presence and hormonal regulation of protein phosphatase inhibitor-1 in ventricular cardiomyocyte. *Am J Physiol Heart Circ Physiol* **270**, H1159–H1164.

Hartzell HC (1988). Regulation of cardiac ion channels by catecholamines, acetylcholine and second messenger systems. *Prog Biophys Mol Biol* **52**, 165–247.

Hartzell HC & Rinderknecht A (1996). Calphostin C, a widely used protein kinase C inhibitor, directly and potently blocks L-type Ca channels. *Am J Physiol Cell Physiol* **270**, C1293–C1299.

He J-Q, Pi Y, Walker JW & Kamp TJ (2000). Endothelin-1 and photoreleased diacylglycerol increase L-type Ca^{2+} current by activation of protein kinase C in rat ventricular myocytes. *J Physiol* **524**, 807–820.

Herzig S & Neumann J (2000). Effects of serine/threonine protein phosphatases on ion channels in excitable membranes. *Physiol Rev* **80**, 173–210.

Hescheler J, Kameyama M, Trautwein W, Mieskes G & Soling H-D (1987). Regulation of the cardiac calcium channel by protein phosphatases. *Eur J Biochem* **165**, 261–266.

Hescheler J, Mieskes G, Ruegg JC, Takai A & Trautwein W (1988). Effects of a protein phosphatase inhibitor, okadaic acid, on membrane currents of isolated guinea-pig cardiac myocytes. *Pflugers Arch* **412**, 248–252.

Hirayama Y & Hartzell HC (1997). Effects of protein phosphatase and kinase inhibitors on Ca^{2+} and Cl^- currents in guinea pig ventricular myocytes. *Mol Pharmacol* **52**, 725–734.

Hu K, Mochly-Rosen D & Boutjdir M (2000). Evidence for functional role of εPKC isozyme in the regulation of cardiac Ca^{2+} channels. *Am J Physiol Heart Circ Physiol* **279**, H2658–H2664.

Kamp TJ & Hell JW (2000). Regulation of cardiac L-type calcium channels by protein kinase A and protein kinase C. *Circ Res* **87**, 1095–1102.

Kelso E, Spiers P, McDermott B, Scholfield N & Silke B (1996). Dual effects of endothelin-1 on the L-type Ca^{2+} current in ventricular cardiomyocytes. *Eur J Pharmacol* **308**, 351–355.

Kurata S, Ishikawa K & Iijima T (1999). Enhancement by arginine vasopressin of the L-type Ca^{2+} current in guinea pig ventricular myocytes. *Pharmacol* **59**, 21–33.

McHugh D, Sharp EM, Scheuer T & Catterall WA (2000). Inhibition of cardiac L-type calcium channels by protein kinase C phosphorylation of two sites in the N-terminal domain. *Proc Natl Acad Sci U S A* **97**, 12334–12338.

Marx SO, Reikin S, Hisamatsu Y, Gaburjakova M, Gaburjakova J, Yang Y-M, Rosemblit N & Marks AR (2001). Phosphorylation-dependent regulation of ryanodine receptors: a novel role for leucine/isoleucine zippers. *J Cell Biol* **153**, 699–708.

Mochly-Rosen D, Wu G, Hahn H, Osinska H, Liron T, Lorenz JN, Yatani A, Robbins J & Dorn II GW (2000). Cardiotrophic effects of protein kinase Cε: analysis by in vivo modulation of PKCε translocation. *Circ Res* **86**, 1173–1179.

Naraghi M & Neher E (1997). Linearized buffered Ca^{2+} diffusion in microdomains and its implications for calculation of $[Ca^{2+}]$ at the mouth of a calcium channel. *J Neurosci* **17**, 6961–6973.

Neumann J, Boknik P, Herzig S, Schmitz W, Scholz H, Gupta RC & Watanabe AM (1993). Evidence for physiological functions of protein phosphatases in the heart: evaluation with okadaic acid. *Am J Physiol Heart Circ Physiol* **265**, H257–H266.

Neumann J, Boknik P, Herzig S, Schmitz W, Scholz H, Wiechen K & Zimmermann N (1994). Biochemical and electrophysiological mechanisms of the positive inotropic effect of calyculin A, a protein phosphatase inhibitor. *J Pharm Exp Ther* **271**, 535–541.

Neumann J, Eschenhagen T, Jones LR, Linck B, Schmitz W, Scholz H & Zimmermann N (1997). Increased expression of cardiac phosphatases in patients with end-stage heart failure. *J Mol Cell Cardiol* **29**, 265–272.

Ono K & Fozzard HA (1993). Two phosphatase sites on the Ca^{2+} channel affecting different kinetic functions. *J Physiol* **470**, 73–84.

Piacentino V III, Dipla K, Gaughan JP & Houser SR (2000). Voltage-dependent Ca^{2+} release from the SR of feline ventricular myocytes is explained by Ca^{2+}-induced Ca^{2+} release. *J Physiol* **523**, 533–548.

Rothermel JD & Parker-Botelho LH (1988). A mechanistic and kinetic analysis of the interactions of the diastereoisomers of adenosine 3′,5′-(cyclic) phosphorothioate with purified cyclic AMP-dependent protein kinase. *Biochem J* **251**, 757–762.

Santana LF, Chase EG, Votaw VS, Nelson MT & Greven R (2002). Functional coupling of calcineurin and protein kinase A in mouse ventricular myocytes. *J Physiol* **544**, 57–69.

Schröder F, Handrock R, Beuckelmann DJ, Hirt S, Hullin R, Priebe L, Schwinger RHG, Weil J & Herzig S (1998). Increased availability and open probability of single L-type calcium channels from failing compared with nonfailing human ventricle. *Circ* **98**, 969–976.

Shistik E, Ivanina T, Blumenstein Y & Dascal N (1998). Crucial role of N terminus in function of cardiac L-type Ca^{2+} channel and its modulation by protein kinase C. *J Biol Chem* **273**, 17901–17909.

Silberman SR, Speth M, Nemani R, Ganapathi MK, Dombradi V, Paris H & Lee YCE (1984). Isolation and characterization of rabbit skeletal muscle protein phosphatases C-I and C-II. *J Biol Chem* **259**, 2913–2922.

Tada M & Katz AM (1982). Phosphorylation of the sarcoplasmic reticulum and sarcolemma. *Ann Rev Physiol* **44**, 401–423.

Trautwein W & Hescheler J (1990). Regulation of cardiac L-type calcium current by phosphorylation and G proteins. *Ann Rev Physiol* **52**, 257–274.

Tseng G-N & Boyden PA (1991). Different effects of intracellular Ca and protein kinase C on cardiac T and L Ca currents. *Am J Physiol Heart Circ Physiol* **261**, H364–H379.

Vinogradova TM, Zhou Y-Y, Bogdanov KY, Yang D, Kuschel M, Cheng H & Xiao R-P (2000). Sinoatrial node pacemaker activity requires Ca^{2+}/calmodulin-dependent protein kinase II activation. *Circ Res* **87**, 760–767.

Walsh AH, Cheng A & Honkanen RE (1997). Fostriecin, an antitumor antibiotic with inhibitory activity against serine/threonine protein phosphatases types 1 (PP1) and 2A (PP2A), is highly selective for PP2A. *FEBS Let* **416**, 230–234.

Wang YG & Lipsius SL (1995). Acetylcholine elicits a rebound stimulation of Ca^{2+} current mediated by pertussis toxin-sensitive G protein and cAMP-dependent protein kinase A in atrial myocytes. *Circ Res* **76**, 634–644.

Wiechen K, Yue DT & Herzig S (1995). Two distinct functional effects of protein phosphatase inhibitors on guinea-pig cardiac L-type Ca^{2+} channels. *J Physiol (Lond)* **484**, 583–592.

Woo S-H & Lee CO (1999). Effects of endothelin-1 on Ca^{2+} signaling in guinea-pig ventricular myocytes: role of protein kinase C. *J Mol Cell Cardiol* **31**, 631–643.

Wu Y, MacMillan LB, McNeill RB, Colbran RJ & Anderson ME (1999). CaM kinase augments cardiac L-type Ca^{2+} current: a cellular mechanism for long Q-T arrhythmias. *Am J Physiol Heart Circ Physiol* **276**, H2168–H2178.

Xiao R-P, Cheng H, Lederer WJ, Suzuki T & Lakatta EG (1994). Dual regulation of Ca^{2+}/calmodulin-dependent kinase II activity by membrane voltage and by calcium influx. *Proc Natl Acad Sci U S A* **91**, 9659–9663.

Yabe K, Ishishita H, Tanonaka K & Takeo S (1998). Pharmacologic preconditioning induced by β-adrenergic stimulation is mediated by activation of protein kinase C. *J Cardiovasc Pharmacol* **32**, 962–968.

You Y, Pelzer DJ & Pelzer S (1997). Modulation of L-type Ca^{2+} current by fast and slow Ca^{2+} buffering in guinea pig ventricular cardiomyocytes. *Biophys J* **72**, 175–187.

Yuan W & Bers DM (1994). Ca-dependent facilitation of cardiac Ca current is due to Ca-calmodulin-dependent protein kinase. *Am J Physiol Heart Circ Physiol* **267**, H982–H993.

Yuan W & Bers DM (1995). Protein kinase inhibitor H-89 reverses forskolin stimulation of cardiac L-type calcium current. *Am J Physiol Cell Physiol* **268**, C651–C659.

Acknowledgements

This work was supported in part by National Institutes of Health Grants PO1 HL-70709 and AG-14637.